ISSN 1027-5495. Functional Materials, 29, No.1 (2022), p. 81-92.
doi:https://doi.org/10.15407/fm29.01.81

Influence of twist extrusion and thermal action on texturing and properties of titanium

***V.V.Usov*[1], *N.M.Shkatuliak*[1], *Ye.S.Savchuk*[1], *N.I.Rybak*[1], *D.V.Pavlenko*[2], *D.V.Tkach*[2], *O.M.Khavkina*[2]**

[1]South Ukrainian National Pedagogical University named after K.Usyinsky, 26 Staroportofrankovskaya Str., 65020 Odesa, Ukraine
[2]Zaporozhye Polytechnic National University, 64 Zhukovskogo Str, 69063 Zaporozhye, Ukraine

Received July 7, 2021

Changes in the elastic modulus, hardness, and ultimate strength of commercially pure titanium (Titanium Grade 2) were studied depending on the direction of severe plastic deformation and subsequent heat treatment of the sample. Severe plastic deformation (SPD) was performed by twist extrusion. Heat treatment was carried out by annealing in the temperature range of 200–400°C with an interval of 50°C. The use of SPD led to the grain refinement to an average size of 200...500 nm from 150...300 μm in the initial state. The change in physical and mechanical properties was associated with the development of a crystallographic texture represented by the Kearns texture parameters, which show the degree of coincidence of the *c*-axes of the crystalline hexagonal cell of grains with a given geometric direction in a polycrystalline material. The texture of the samples was investigated using the X-ray method by constructing reverse pole figures. It has been shown that the anisotropy of th e elastic modulus after SPD was about 14.0 %. With an increase in the annealing temperature, the anisotropy decreased. After annealing at 250°C, the Kearns texture parameters had the closest values corresponding to the tex ture less state. With a further increase in the annealing temperature, the anisotropy of the elastic modulus increased; after annealing at 400°C its value was 16.42 %. Based on the empirical ratios of hardness and strength of single crystals in titanium of technical purity, the values of the ultimate strength and yield strength of a titanium single crystal along its hexagonal axis and in the direction perpendicular to it were found. The anisotropy coefficients of the ultimate strength and yield streng th of titanium after SPD were determined. The regularity of their change in connection with the temperature of the subsequent annealing was established.

Keywords: titanium, severe plastic deformation, twist extrusion, heat treatment, crystallographic texture, pole figure, anisotropy, elastic modulus, ultimate strength, hardness.

Вплив гвинтової екструзии та температури на текстуроутворення й властивості титана. *В.В.Усов, Н.М.Шкатуляк, Е.С.Савчук, Н.И.Рибак, Д.В.Павленко, Д.В.Ткач, О.М.Хавкына*

Досліджували зміни модуля пружності, твердості й межі міцності технічно чистого титану (Titanium Grade 2) залежно від напрямку в зразку, підданого інтенсивної пластичної деформації (ІПД) й наступної термічної обробки. Інтенсивну пластичну виконували методом гвинтової екструзії. Термічну обробку виконували шляхом відпалу в діапазоні температур 200–400°С с інтервалом в 50°С. Застосування ІПД призвело до здрібнювання зерен від середнього розміру 150 300 мкм у вихідному стані до 200...500 нм. Зміна фізичних і механічних властивостей зв'язували з розвитком кристалографічної текстури, представленої параметрами текстури Кернса, які показують ступінь збігу *с*-осей кристалічного гексагонального гнізда зерен із заданим

геометричним напрямком у полікристалічному матеріалі. Текстуру зразків досліджували рентгенівським методом шляхом побудови зворотних полюсних фігур. Показане, що анізотропія модуля пружності після ІПД склала порядку 14,0 %. З ростом температури відпалу анізотропія зменшувалася. Після відпалу при 250°С параметри текстури Кернса мали найбільше близькі значення, що відповідають безтекстурному стану. При подальшому збільшенні температури відпалу анізотропія модуля пружності зростала й після відпалу при 400°С її величина прийняла значення 16,42 %. Грунтуючись на емпіричних співвідношеннях твердості й міцності монокристалів титану технічної чистоти, знайдені значення меж міцності й плинності монокристала титану уздовж його гексагональної осі й у перпендикулярному до неї напрямку. Визначені значення коефіцієнтів анізотропії меж міцності й плинності титану після ІПД. Установлена закономірність їх зміни у зв'язку з температурою наступного відпалу.

1. Introduction

Titanium and its alloys have rather low density and high specific strength, which ensures a reduction in product weight. Due to these properties, titanium alloys are widely used in the aircraft and space industries. Like most metals and alloys with a hexagonal crystal structure, titanium becomes highly anisotropic during machining. This circumstance often limits its practical use. For example, metal consumption increases during stamping or deep drawing. One of the main reasons for the titanium prop erties anisotropy is its crystallographic texture.

However, the texture can cause not only defects in products. The creation of a certain texture in a metallic material can significantly increase the strength of products. For example, the creation of a favorable texture in titanium alloys makes it possible to increase the deformation resistance under biaxial tension by 45 % compared to uniaxial one [1]. At the same time, solving the problem of designing machine parts associated with the choice of their correct orientation is especially important for titanium alloys. Considering that during the manufacturing process, as well as during operation, the material is exposed to thermal effects, which can lead to structural changes, the assessment of its effect on texture formation is also of great applied importance. Thus, the study and search for the conditions for formation of the favorable crystallographic texture during the processing of titanium and its alloys is relevant.

An important factor for improving the properties of metallic materials including titanium and its alloys is the creation of a deformation sub-microcrystalline structure in parts made of them. This structure makes it possible to significantly increase the strength properties without deteriorating the metal ductility. The formation of a sub-microcrystalline deformation structure (SMDS) in the metal occurs under the action of severe plastic deformation (SPD). In practice, various SPD technologies are used [2]. One of these methods is twist extrusion (TE). The titanium texture formation during TE was investigated in [3, 4]. In these and a number of other papers, it was shown that the texture formation during TE can be caused not only by the action of basic, prismatic, and pyramidal sliding and twinning, but also qby the vortex motion of being refined fragments of the grains that is similar to a turbulent fluid flow.

The peculiarity of the metal flow during SPD also predetermines a number of texturing features in comparison with well-studied methods of pressure shaping. At the same time, the currently available research results in this area are often contradictory. This makes it difficult for designers and technologists to make an applied assessment of the strength reliability for products made of the materials with the sub-microcrystalline structure and designing blanks for them.

According to the authors of [5], the features of texture formation in the SPD process in metals with a hexagonal-close-packed (HCP) lattice have not been studied completely. They studied the effect of the deformation rate and temperature on the texture of commercially pure titanium and showed that for the selected deformation mode, the basal plane (0001) forms an angle of 45© to the compression axis. In [6], the authors showed that the commercially pure titanium texture formed by rolling significantly affects the features of its plastic deformation and, accordingly, the deformation anisotropy.

The SPD effect on the crystallographic texture was studied in [7]. It was found that during severe deformation and subsequent rolling, a significant anisotropy of mechanical properties is formed. According to the authors, in addition to the effect of the crystallographic texture that appears

Table 1. Chemical composition of commercially pure titanium, wt.%

VT1-0 (GOST 19807-91)						
C	Si	N	Fe	O	H	Ti
<0. 07	<0.1	<0.04	<0.25	<0.2	<0.2	Rest
Titanium Grade2						
C	H	O	N	Fe	Ti	
<0.08	<0.015	<0.25	<0.03	<0.30	Rest	

during deformation, the oriented deformation substructure also makes a significant contribution to the anisotropy of properties. In [8], it was established that the plastic deformation mechanisms and crystallographic texture depend on the deformation magnitude. The processing method also significantly affects the features of the texture. In particular, the titanium texture formed as a result of equal-channel angular extrusion had characteristic features for each processing route [9]. However, the relationship between the texture parameters and the elastic and mechanical characteristics of the VT1-0 titanium alloy after twist extrusion has not been sufficiently studied. Available publications on the texture formation of VT1-0 (Titanium Grade 2) titanium alloy by the twist extrusion method are also based on simplified methods [4], which do not allow reliable assessing the processes occurring in the material during SPD.

The aim of this work was to establish the patterns of texture formation in the billet during twist extrusion and to study the effect of the crystallographic texture on the elastic modulus and mechanical characteristics of titanium after SPD and additional heat treatment.

2. Expeimental

The studies were carried out on commercially pure VT1-0 titanium, which roughly corresponds in chemical composition to Titanium Grade2 alloy (Table 1).

The billets made of VT1-0 (Titanium Grade 2) titanium and subjected to SPD by the TE method were investigated [2]. An alloy billet was placed in a matrix with a helical channel of rectangular cross section with an angle of the helix inclination to the TE axis (Fig. 1).

The billet length was 70 mm, and the section was 18×28 mm. The extrusion pressure was p_1 = 1600 MPa. To increase the technological plasticity of the titanium alloy, back pressure was applied to the front

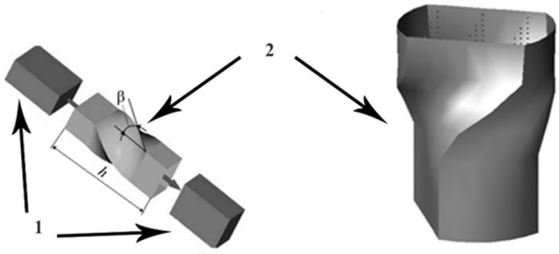

Fig. 1. Scheme of the twist extrusion [10]: 1 — billet: 2 — helical channel of the TE rigging.

end of the billet, the value of which was p_2 = 200 MPa; mixture based on low-melting glass was also used.

The total relative shear deformation Λ per pass can be calculated by the formula [2]:

$$\Lambda = \frac{2}{\sqrt{3}} \cdot \mathrm{tg}\gamma_{\max}, \qquad (1)$$

where γ_{max} is the maximum angle of inclination between the twist line and the extrusion axis.

The calculation showed that the total shear deformation per pass is approximately 1.15. Five TE passes were carried out. Thus, the total relative shear deformation of the billet was 5.77.

The billets were preheated in a furnace to a temperature of t = 400°C. The average size of the structural components (grains and subgrains) in the samples after five TE passes was in the range of 200...500 nm. The size of the structural components in the original samples was 150...300μm.

After extrusion, samples were cut from the billet by the electroerosive qmethod. The samples were cubes with dimensions 10×10×10 mm. One of the cube edges was oriented along the pressing axis (TE axis), and the other two, respectively, were perpendicular to the above axis. The samples after TE were subjected to isochronous vacuum annealing for 1 hour at temperatures of 200, 250, 300, 350, and 400°C.

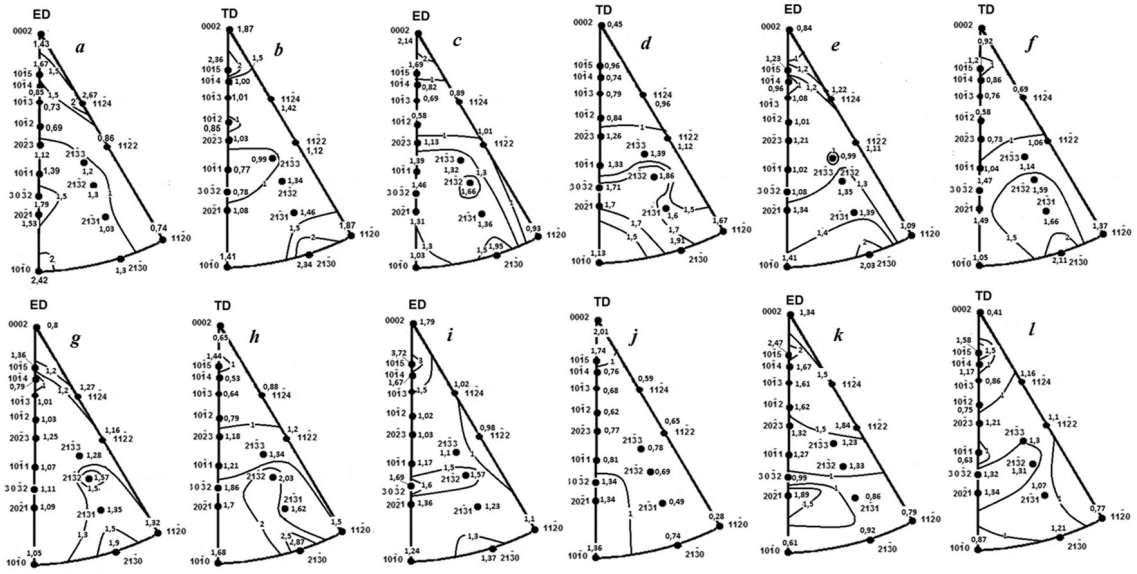

Fig. 2. Inverse pole figures of VT1-0 titanium alloy samples after five passes of twist extrusion (a, b) and after annealing at temperatures of 200 (c, d), 250 (e, f), 300 (g, h), 350 (i, j) and 400°C (k, l), respectively.

The texture of the samples after extrusion, as well as after annealing, was studied by the X-ray method. Before examining their texture, the samples were chemically polished to a depth of 0.1 mm to remove the surface layer distorted by the cutout. θ–2θ scanning was performed on a diffractometer in Mo–K_α radiation according to the Bragg-Brentano geometry [11]. Based on the results of diffractometry analysis, inverse pole figures (IPF) in the TE axis direction (Extrusion Direction) — ED IPF, and in the direction perpendicular to the extrusion axis (Transverse Direction) — TD IPF were constructed. When drawing the IPF, the Morris normalization was used [12].

3. Results and discussion

Fig. 2 shows the inverse pole figures of the samples in the extrusion axis direction (ED IPF) and in the direction perpendicular to the extrusion axis direction (TD IPF) after five TE passes and after annealing at the temperatures indicated above.

The texture after five extrusion passes can be generally described as the distribution of the crystallite hexagonal axes within the cone-shaped surfaces described around the extrusion axis with half opening angles from 0 to 38.5 degrees and 50 to 90 degrees. On the whole, the pole density distribution on the TD IPF after five TE passes looks like a fan-shaped scatter of crystal orientations, which was indicated in the earlier paper on the study of the crystallographic texture in the VT1-0 alloy after TE [3]. This may prove that, in addition to the crystallographic mechanisms (basic, prismatic, and pyramidal sliding and twinning), the vortex nature of the movement of crystallites during their fragmentation contributes to the texture formation in the TE process. Such a movement resembles the fluid turbulent motion in its turbulent flow [13, 14].

Annealing of the extruded VT1-0 sample at 200°C generally reduces the value of the pole density at the IPF (Fig. 3, c, d). The texture character changed a little. The maximum of 2.14 on the ED IPF has moved from the pole ⟨11$\bar{2}$4⟩, where it was after the TE, to the pole ⟨0002⟩. As a result, after annealing at 200°C, the hexagonal axes of the qcrystallites are distributed within the cone-shaped surfaces around the extrusion axis, but with half-opening angles from 0 to 25 degrees and from 50 to 90 degrees.

An increase in the annealing temperature to 250°C promotes the redistribution of the pole density on the IPF (Fig. 3, e, f). One maximum at the ED IPF (Fig. 3, e) seems to be "blurred" from the pole ⟨10$\bar{1}$5⟩ with an intensity of 1.23 to the pole ⟨11$\bar{2}$4⟩ with an intensity of 1.22. The second pole density maximum of 2.08 is observed at the pole ⟨21$\bar{3}$0⟩. Moreover, the pole density scattering region occupies almost the entire stereographic triangle. On the whole, the hexagonal axes of the crystallites are distributed inside a truncated cone-shaped sur-

face described around the extrusion axis. The angles qof the half opening of the conical surface vary in the range from 20 to 90 degrees. Annealing at a temperature of 300°C has little changed the distribution of hexagonal crystallite axes relative to the extrusion axis (Fig. 2, g, h). Their distribution is practically similar to its picture after annealing at 250°C. After annealing at 350°C and 400°C, the distribution density of the crystallite hexagonal axes oriented near the extrusion axis (inside the conical surfaces with a half-opening angles from 0 to 20 degrees) slightly increased. On the whole, the distribution of the directions of the crystallite hexagonal axes both after extrusion and after annealing resembles a fan-shaped spread of their orientations relative to the extrusion axis as was mentioned above.

It is known, that during annealing the processes of recovery and recrystallization in metals are observed [15]. The recovery occurs at relatively low temperatures (below $0.3T_{melt}$ [15]). No significant structural changes occur at the first stage of the recovery, however, in this case the residual stresses decrease and the plasticity increases. At the second stage of recovery (polygonization), new low-angle boundaries are formed within each crystal. As a result, the crystal is fragmented into subgrains (polygons). However, polygonization in pure metals is observed after slight deformation [16].

At higher annealing temperatures, a recrystallization process occurs — i.e. the process of nucleation and growth of new undistorted grains. Bochvar found [15] that the absolute recrystallization temperature T_{recr} for pure metals is approximately 0.4 of the melting temperature T_{melt}, that is:

$$T_{recr} \approx 0.4T_{melt} \qquad (2)$$

Thus, the calculated temperature of the onset of recrystallization for pure titanium is approximately 500°C. However, a decrease in the purity of the metal, as well as an increase in the degree of deformation, contributes to a decrease in the recrystallization temperature [17].

The data on the recrystallization temperature for titanium after SPD differ. For example, authors of [18] studied the effect of annealing on the structure of commercial Titanium Grade2 after SPD by the hydraulic extrusion (HE) in three passes with a total true relative plastic deformation of 2.75. It was shown that the temperature of the recovery onset decreased from ~ 480°C in the starting material to ~ 280°C after hydraulic extrusion (i.e., by 70 %). The recrystallization onset temperature dropped from 660°C to 570°C (i.e., by 15 %, respectively).

To compare other published data, we can mention the results [19] obtained using differential scanning calorimetry in titanium treated with the equal channel angular pressing (ECAP) method. The analysis showed that after 3 passes, the recovery onset temperature decreased from 440°C after one ECAP pass to 310°C, that is, by 40 %. Comparing this result with the one obtained in the previous work [18], it can be seen that SPD with the help of HE has a greater effect on the decrease in the temperature of the onset of reduction and recrystallization.

Earlier it was reported that the onset temperature recrystallization in Titanium Grade 2 was 527°C after 8 ECAP passes [20]. In [21], the thermal stability of the VT1-0 alloy structure after SPD was investigated by the TE method. The extrusion pressure was 2400 MPa, the back pressure was 200 MPa, and the temperature was 350°C. There were five TE passes. It was shown that during annealing in the temperature range of 300–350°C, recovery processes occur; and after annealing at 385°C, the first diffraction reflections appeared, which indicated that the first recrystallized grains started to form, which means the beginning of recrystallization.

Since the SPD of the investigated samples of the VT1-0 alloy was carried out using the TE method, as in the above-mentioned paper, it can be assumed that during annealing, similar phenomena are observed at the corresponding temperatures in the samples.

For a more objective quantitative assessment of the texture and its effect on the bulk physical and mechanical properties of hexagonal materials, the Kearns texture coefficients are used [22, 23]. These coefficients f_j (index j means the corresponding direction in the sample, in this case ED or TD) show the degree of coincidence of the c-axes of the crystalline hexagonal cell of grains with a given geometric direction in a polycrystalline material and can be found from the IPF according to the ratio:

$$f_j = \langle \cos^2\alpha_j \rangle_j = \sum_i A_j P_{ji} \cos^2\alpha_i, \qquad (3)$$

where $P_{ji} = \frac{I_i/I_R}{\sum_{\Delta} (A_i \cdot I_i/I_R)}$ is the pole density at the IPF; I_i/I_R is the the ratio of the integral intensity of the i-th reflection on the j-th IPF to the corresponding value of the reflex of the sample without texture; A_i are the statistical weights of the i-th reflex ($\sum A_i P_{ji} = 1$) [24].

Conditionally, A_i is determined by the fraction of the surface area of the stereographic triangle around the normal to the i-th reflex of the corresponding IPF; α_i is the angle of deviation of the i-th crystallographic direction from the c-axis for the j-th direction in the sample. For single hexagonal crystals:

$$P(\varphi)_{ref} = P_c \cos^2\varphi + P_a(1 - \cos^2\varphi). \quad (4)$$

where $P(\varphi)_{ref}$ is the property in the chosen direction, P_a and P_c are the properties of the single crystal in the direction perpendicular and parallel to the direction [0002], respectively, φ is the angle between the chosen direction and [0002].

Assuming that crystallites in a polycrystal contribute to the volumetric property in proportion to their volume fraction, V_i, the contribution to the volumetric property of crystals, whose axes are oriented at an angle of inclination φ to the chosen direction, can be written as:

$$P(\varphi_i)_{ref} = P_c V_i \cos^2\varphi_i + P_a V_i(1 - \cos\varphi_i). \quad (5)$$

Summing over the entire volume, we get:

$$P(\varphi_i)_{ref} = P_c \sum_i V_i \cos^2\varphi_i + P_a \sum_i V_i(1 - \cos\varphi_i). \quad (6)$$

Since $\sum_i V_i = 1$, and $\sum_i V_i \cos^2\varphi_i =$ is the Kearns texture parameter, we can write:

$$P(\varphi_i)_{ref} = f_j P_c + (1 - f_j) P_a. \quad (7)$$

To find the Kearns texture coefficients, we used the IPF in Fig. 2. The values A_i were taken from [24]. The angles α_i were calculated by the known formulas [26] taking into account the ratio of the crystal lattice parameters of the alloy under study $c/a = 1.587$.

Kerns showed [22] that if a material property can be described by a tensor (such as elasticity), then it obeys relation (7). In this case, the sum in the three main directions of the sample should be equal to one, and a value of 1/3 in each direction determines the isotropic case. Thus, if the Kearns texture coefficients found from ED IPF (f_{ED}) and TD IPF (f_{TD}) are known, we can find the Kearns coefficient for the third direction in the sample after extrusion — the radial direction (RD) — by the ratio:

$$f_{ED} + f_{TD} + f_{RD} = 1. \quad (8)$$

Kearns texture coefficients calculated from ED IPF (f_{ED}) and TD IPF (f_{TD}) in Fig. 2 as well as those calculated by relation (8), are given in Table 2.

It can be seen from Table 1 that after annealing at 250°C, the Kearns texture coefficients are closest to 1/3. According to Kearns [22], the value of the coefficients 1/3 in each direction means the isotropic case, as mentioned above. It will be shown below that after annealing the extruded sample at 250°C, the anisotropy of the investigated properties is minimal (Table 4, 6).

The experimental determination of the elastic and strength properties in the longitudinal direction (in the direction of the TE axis) of the VT1-0 titanium alloy after 5 TE passes was previously carried out in [27]. Due to the rather small cross-section of the billet (18×28) mm, the measurements of the above properties in the transverse direction after TE are difficult. We estimated the values of Young's modulus of the VT1-0 titanium alloy after five passes of deformation by TE and subsequent annealing in the direction of the extrusion axis and in the transverse direction according to relation (7), using the Kearns texture coefficients (Table 2) and the values of the corresponding properties of single crystals. Table 3 shows the results of measurements made by various authors for the elastic moduli of single crystals of commercial titanium similar in chemical composition to the investigated alloy VT1-0. It is seen from Table 3, the experimental results on the elastic properties of single crystals published by various authors differ.

To estimate the values of the elastic modulus of investigated samples in the direction of the extrusion axis (ED) and in the transverse direction (TD), we will use the averaged values of the elastic moduli of a titanium single crystal from Table 3 and calculate the modulus of elasticity by the ratios:

$$E_{ED} = f_{ED} \cdot E_c^{av} + (1 - f_{ED}) \cdot E_a^{av}, \quad (9)$$

Table 2. Kearns texture coefficients after 5 passes of twist extrusion and subsequent annealing of VT1-0 titanium alloy

Annealing temperature, °C	f_{ED}	f_{TD}	f_{RD}
after 5 TE passes	0. 488	0.471	0.041
200	0.406	0.363	0.231
250	0.391	0.334	0.275
300	0.407	0.376	0.217
350	0.578	0.325	0.097
400	0.565	0.393	0.042

$$E_{TD} = f_{TD} \cdot E_c^{av} + (1 - f_{TD}) \cdot E_a^{av}, \quad (10)$$

$$E_{RD} = f_{RD} \cdot E_c^{av} + (1 - f_{RD}) \cdot E_a^{av}. \quad (11)$$

The calculation results are presented in Table 4.

The anisotropy coefficient η was estimated by the ratio:

$$\eta = [(F_{\max} - F_{\min})/F_{\min}] \cdot 100\%, \quad (12)$$

where F is the corresponding property.

The anisotropy coefficient of the elastic modulus η decreases with an increase in the annealing temperature up to 250°C (Table 4). After annealing at 250°C, the anisotropy coefficient of the elastic modulus takes on a minimum value of 3.35 %. With a further increase in the annealing temperature, the anisotropy coefficient of the elastic modulus increases and after annealing at 400° it takes on a maximum value of 16.42 %. An increase in the anisotropy coefficient η after annealing at temperatures above 250°C is probably associated with recrystallization processes and as a consequence, a change in the texture of the samples.

According to the data of [27], the experimental value of the elasticity modulus in the direction of the extrusion axis for the VT1-0 titanium alloy after 5 passes of TE was E = 113.0 GPa. This value is about 9.4 % less than our estimated value E = 123.6 GPa (Table 4). This discrepancy may be due to the fact that the result in [27] was obtained by uniaxial elastoplastic tension to the level of plastic deformation ε = 0.007, followed by unloading and again loading. With this method of deformation, microdefects (for example, vacancies, interstitial atoms, possibly, micropores) can be formed in the material. The accumulation of microdefects reduces the effective bearing load of the sample cross-sectional area, which leads to a decrease in the elastic modulus [32].

Table 3. Elastic properties of titanium single crystals

E_c, GPa	E_a
143	122
130	97
146	103
146	104
$E_c^{av} \approx 141$	$E_a^{av} \approx 107$

Let us estimate the ultimate strength and yield strength of the VT1-0 titanium alloy after TE and annealing according to the data for a single crystal. For this purpose, let us first estimate the ultimate strength and yield strength of a single crystal of the VT1-0 alloy along the c axis as well as along the a axis. There are no such data in the literature. However, they can be found using hardness data from nanoindentation results. These results vary significantly d epending on the titanium purity. For high-purity titanium (iodide titanium, HP Ti, CP Ti (grade 1)), the minimum value of hardness was found at nanoindentation of the basal plane [33, 34]. At the same time, in titanium of lower purity, for example, in the VT1-0 or CP Ti (grade 2) alloy under study, the basal plane is the hardest [35–37]. Table 5 shows the results of measuring the hardness for nanoindentation along the c-axis (H_V^c), and along the a-axis (H_V^a), obtained by differe nt authors for single crystals of titanium of technical purity, similar to VT1-0.

The results of nanoindentation obtained by different authors differ (Table 5). Therefore, for further calculations, we will use the corresponding averaged values H_V^c and H_V^a for the titanium single crystal. We will estimate the values σ_B^c and σ_B^a of the corresponding ultimate strength according to the empirical relations [38], which, taking into account the measurements in MPa and minor transformations, have the form:

$$H_V \approx 2.89\sigma_B, \quad (13)$$

$$H_V \approx 3.33\sigma_{0.2}, \quad (14)$$

where H_V is the Vickers hardness.

Table 4. Elastic moduli of VT1-0 titanium alloy calculated using Kearns texture coefficients (Table 2) and elastic moduli of a single crystal (Table 3)

Annealing temperature, °C	E_{ED},	GPa	E_{TD}, GPa	E_{RD}, GPa
after 5 TE passes	123.6	123.0	108.4	14.0
200	120.8	119.3	114.0	5.96
250	120.3	118.4	116.4	3.35
300	120.8	119.8	114.4	5.59
350	126.7	118.1	110.3	14.87
400	126.2	120.4	108.4	16.42

Using relation (13), (14), and the values and from Table 5, we get:

$$\sigma_B^c = 615MPa, \quad \sigma_{0.2}^c = 534MPa, \qquad (15)$$

$$\sigma_B^a = 356MPa; \quad \sigma_{0.2}^a = 308MPa. \qquad (16)$$

To assess the ultimate strength of the VT1-0 alloy after 5 passes of the TE and annealing, we use relationships similar to (9)–(11):

$$\sigma_B^{ED} = f_{ED} \cdot \sigma_c + (1 - f_{ED}) \cdot \sigma_a, \qquad (17)$$

$$\sigma_B^{TD} = f_{TG} \cdot \sigma_c + (1 - f_{TD}) \cdot \sigma_a, \qquad (18)$$

$$\sigma_B^{RD} = f_{RD} \cdot \sigma_c + (1 - f_{RD}) \cdot \sigma_a. \qquad (19)$$

Similarly for the yield point, we get:

$$\sigma_{0.2}^{ED} = f_{ED} \cdot \sigma_c + (1 - f_{ED}) \cdot \sigma_a, \qquad (20)$$

$$\sigma_{0.2}^{TD} = f_{TD} \cdot \sigma_c + (1 - f_{TD}) \cdot \sigma_a, \qquad (21)$$

$$\sigma_B^{RD} = f_{RD} \cdot \sigma_c + (1 - f_{RD}) \cdot \sigma_a. \qquad (22)$$

The calculation results are presented in Table 6. From Table 6 it can be seen that there is anisotropy of mechanical characteristics. In this case, the ultimate strength and yield strength have a maximum value along the extrusion axis. The anisotropy indices (η) of the characteristics σ_B and $\sigma_{0.2}$ take their minimum values after annealing at 250°C. An increase in the anisotropy coefficients after annealing at 250°C is probably due to changes in the texture of the samples during recrystallization.

In [27], the values of the ultimate strength and yield strength obtained under uniaxial tension along the TE axis of the VT1-0 titanium alloy after 5 TE passes (Λ = 5.77) were σ_B^{ED} = 475 MPa and $\sigma_{0.2}^{ED}$ = 412 MPa. The corresponding estimated values obtained by us (Table 6) are approximately 1.5 % and 1.7 %, respectively, higher than the experimental data presented in [27].

Table 5. Titanium single crystal hardness

H_V^c, GPa	H_V^a	GPa
2.73	1.34	[35]
1.0	0.75	[36]
1.6	1.0	[37]
H_{Vcp}^c = 1.78	H_{Vcp}^a = 1.03	

The results of microhardness H_μ measurements of investigated Ti samples at a load of 5 N and a load time of 10 sec, as well as standard deviations (SD), are presented in Table 7.

It can be seen that the ratio of microhardness H_μ to ultimate strength and tensile yield in the VT1-0 titanium alloy after TE does not obey empirical relations (11) and (12), which are valid for those materials that have a conventional rather than sub-microcrystalline structure.

In [38, 39], the relationship between hardness and yield strength and tensile strength, as well as the shape of indentations of the indenter were analyzed, when determining the hardness H_V for various materials. The authors of [38] classified the indentation geometry into three types:

a) "contraction" (the shape of the print resembles a square, the sides of which are pulled together, bending towards the center);

b) "pile-up" (a bulge forms around the imprint due to hardening near the imprint);

c) "crack" (local cracking occurs around the print).

The authors of [38] showed that for materials that show indentations of type (a) (materials which have not a sub-microcrystalline structure), one third of the hardness is in the range from yield strength to ultimate tensile strength.

Table 6. Ultimate strength σ_B and yield strengths $\sigma_{0.2}$ of the VT1-0 titanium alloy calculated using the Kearns texture coefficients (Table 2) and the values of σ_B^c and σ_B^a for a titanium single crystal (15), (16)

Annealing temperature, °C	σ_B^{ED}, MPa	$\sigma_{0.2}^{ED}$, MPa	σ_B^{TD}, MPa	$\sigma_{0.2}^{TD}$, MPa	σ_B^{RD}, MPa	$\sigma_{0.2}^{RD}$, MPa	$\eta_{\sigma B}$, %	$\eta_{\sigma 0.2}$, %
–	482	419	478	415	367	319	32.0	32.
200	461	400	450	391	416	361	11.0	11.0
250	457	397	443	384	427	371	7.0	7.0
300	462	401	454	394	412	358	12,0	12.0
350	506	439	440	382	381	331	33.0	33.0
400	502	436	458	397	367	319	37.0	37.0

Table 7. Microhardness H_μ of VT1-0 titanium alloy after 5 TE passes and annealing

Annealing temperature, °C	H_μ^{ED}, MPa	SD, MPa	H_μ^{TD}, MPa	SD, MPa	H_μ^{RD}, MPa	SD, MPa
–	2310	240	2150	90	1830	10
200	2110	40	2100	15	1820	170
250	1910	100	1890	50	1790	90
300	1850	110	1750	80	1670	140
350	1820	130	1660	20	1610	90
400	1780	120	1620	90	1510	60

For materials with an indentation of type (b), (with a sub-microcrystalline structure) the ratio of hardness to ultimate strength is different from 3. Depending on the degree of hardening around the indentation, this ratio can be either less or more than 3. The latter is observed when comparing the data in Tables 6 and 7.

The hardness of materials with indentation morphology of type (b) (brittle materials) is related to fracture behavior, but differs from tensile strength due to different stress states. For such materials, the ratio H_V/σ_B can significantly exceed 3. This may be due to different tensile strengths when tested for hardness and tensile, due to a decrease in the ability to shear and easier cleavage [38, 39].

4. Conclusions and prospects for further research

1. The development of the crystallographic texture of the VT1-0 titanium alloy after 5 passes of twist extrusion and subsequent annealing for 1 hour at temperatures of 200–400°C with an interval of 50°C is represented by the parameters of the Kearns texture, which show the degree of coincidence of the *c*-axes of the crystal hexagonal cell of grains with a given geometric direction in a polycrystalline material.

2. After annealing at 250°C, the parameters of the Kerns texture have the values closest to 1/3 in the three directions of investigated titanium samples. At that, anisotropy of investigated properties is minimal.

3. The evaluation of elastic modulus of the VT1-0 titanium alloy after 5 TE passes and annealing in three mutually perpendicular directions of the samples has been carried out using the Kearns texture parameters and elastic constants of a single crystal of commercial titanium; it showed that the calculated value of the elastic modulus is 9.4 % higher than its experimental value found in [27] from tests for uniaxial tension along the direction of the TE axis. The discrepancymay be due to the peculiarities of the experiment in [27] by elastoplastic deformation to the level of plastic deformation $\varepsilon_{pl} = 0.007$ with subsequent unloading and again loading. In this case, the accumulation of microdefects reduces the effective bearing load of the cross-sectional area of

the sample, which can be the reason for a decrease in the elastic modulus.

4. The anisotropy of the elastic modulus after 5 passes of TE was about 14.0 %. With an increase in the annealing temperature, the anisotropy decreased, and after annealing at 250°C it had a minimum value of 3.35 %. With a further increase in the annealing temperature, the anisotropy of the elastic modulus increased, and after annealing at 400°C its value was 16.42 %.

5. Using empirical relations $H_V \approx 2.89\sigma_B$ and $H_V \approx 3.33\sigma_{0.2}$, as well as the corresponding literature data on hardness H_V^c and H_V^a, obtained by nanoindentation of titanium single crystals of technical purity, the values of the ultimate strength and yield strength of a titanium single crystal were found along its hexagonal axis σ_B^c = 615 MPa, $\sigma_{0.2}^c$ = 534 MPa and in the direction perpendicular to the hexagonal axis σ_B^a = 356 MPa. $\sigma_{0.2}^a$ = 308 MPa.

6. The tensile strength and yield stress in three mutually perpendicular directions of the VT1-0 titanium alloy specimens after 5 passes of TE and annealing were evaluated by means of the Kearns texture parameters and the corresponding values of the tensile strength and yield stress along and across of the titanium single crystal hexagonal axis. The estimated values of the ultimate strength and yield strength along the direction of the TE axis after 5 TE passes by 1.5 an d 1.7 %, respectively, exceed their experimental values obtained in [27] from uniaxial tension tests.

7. The anisotropy coefficients of the ultimate strength and yield strength after 5 passes of TE were about 32.0 %. With an increase in the annealing temperature, the anisotropy of the ultimate strength and yield strength decreased; after annealing at 250°C, the anisotropy coefficients had a minimum value of 7.0 %. With a further increase in the annealing temperature, the anisotropy of the ultimate strength and yield strength increased; after annealing at 400°C, the an isotropy coefficient was 37.0 %.

8. Due to the submicron crystalline deformation structure of VT1-0 titanium after 5 passes of the twist extrusion, the ratios of microhardness to the ultimate strength and yield strength of the alloy exceeds the values obtained from the empirical relations (13) and (14) typical for alloys with a coarse-crystalline structure. As the annealing temperature increases, the aforementioned ratios decrease, approaching empirical values.

Considering that the VT1-0 alloy is very rarely used as a structural material, the prospect of further research is to assess the texture formation and properties of titanium alloys for aerospace purposes. Among the main ones are two-phase and pseudo-two-phase titanium alloys, which are widely used in the production of compressor blades for gas turbine engines.

The established regularities of texture formation and corresponding anisotropy in titanium alloys under the action of torsion extrusion and heat treatment are of great practical importance. Mechanical and physical characteristics of a deformable semi-finished product in various directions are used to assess the strength reliability of parts [40]. Taking into account the established dependence of the ultimate strength and modulus of elasticity on the direction of cutting blanks from a semi-finished product, the number of deformation passes, and the temperature of thermal exposure, the differences in the safety factor of parts can reach 40–50 %. Considering that, for example, for rotor blades of the compressors of gas turbine qengines, the permissible margin of safety is 1.4–1.6, knowledge about the anisotropy of mechanical characteristics is necessary.

References

1. A.I.Khorev, Heat, Thermomechanical Treatment and Textural Hardening of Welded Titanium Alloys [in Russian]. https://www.viam.ru/public/files/2012/2012-206018.pdf
2. Y.Beygelzimer, R.Kulagin, Y.Estrin et al., Advanced Engineering Materials, **19**, ??? (2017), https://www.researchgate.net/publication/316011012_Twist_Extrusion_as_a_Potent_Tool_for_Obtaining_Advanced_Engineering_Materials_A_Review_Twist_Extrusion_as_a_Potent_Tool_for_Obtaining
3. V.V.Usov, N.M.Shkatulyak, P.A.Bryukhanov, Ya.E.Beigelzimer, *Physics and Technology of High Pressures*, **21**, 103 (2011). http://dspace.nbuv.gov.ua/handle/123456789/69437
4. V.E.Olshanetskii, L.P.Stepanova, D.V.Tkach, D.V.Pavlenko, *Met. Sci. Heat Treat,*, **53**, 618 (2012). https://doi.org/10.1007/s11041-012-9445-z
5. Z.Zeng, Y.Zhang, S.Jonsson, *Materials Science and Engineering: A*, **513–514**, 83 (2009). https://doi.org/10.1016/j.msea.2009.01.065
6. J.W.Won, C.H.Park, S.-G.Hong, C.S.Lee, *Journal of Alloys and Compounds*, **651**, 245

(2015).
https://doi.org/10.1016/j.jallcom.2015.08.075
7. G.G.Yapici, I.Karaman, H.J.Maier, *Materials Science and Engineering: A*, **434**, 294 (2006).
https://doi.org/10.1016/j.msea.2006.06.082
8. S.Nourbakhsh, T.D.O'Brien, *Materials Science and Engineering*, **100**, 109 (1988).
https://doi.org/10.1016/0025-5416(88)90245-5
9. S.Suwas, B.Beausir, L.S.Toth et al., *Acta Materialia*, **59**, 1121 (2011).
https://doi.org/10.1016/j.actamat.2010.10.045
10. Y.Beygelzimer, D.Orlov, A.Korshunov et al., *Structures & Material Properties. Solid State Phenomena*, **114**, 69 (2006).
https://hunch.net/~yan/papers/properties.of.twist.extrusion.pdf
11. Instrument X-ray Optics: Reflection Geometry.
http://pd.chem.ucl.ac.uk/pdnn/inst1/optics1.htm
12. P.R.Morris, *Journal of Applied Physics*, **30**, 595 (1959).
https://doi.org/10.1063/1.1702413
13. Y.E.Beygelzimer, Simple Shear and "Turbulence" of Polycrystals.
https://hunch.net/~yan/stati/spd.pdf
14. D.V.Pavlenko, Ya.E.Beygel'zimer, *Powder Metallurgy and Metal Ceramics*, **54**, 517 (2016).
https://link.springer.com/article/10.1007/s11106-016-9744-9
15. K.K.Alaneme, E.A.Okotete, *Journal of Science Advanced Materials and Devices*, **4**, 19 (2019).
https://www.sciencedirect.com/science/article/pii/S2468217918302235#bib49
16. E.Nes, *Acta Metallurgica et Materialia*, **43**, 2189 (1995).,
https://doi.org/10.1016/0956-7151(94)00409-9
17. Metals Grades: Titanium, Alloy and Grades [in Russian],
http://metallicheckiy-portal.ru/marki_metallov/tit
18. J.Skiba, M.Kulczyk, W.Pachla et al., *J. Nanomed. Nanotechnol.*, **9**, ??? (2018)
https://www.longdom.org/open-access/effect-of-severe-plastic-deformation- realized-by-hydrostatic-extrusion-onheat-transfer-in-cp-ti-grade-2-and-316l- austenitic-stainl-2157-7439-1000511.pdf
19. T.Kubina, J.Dlouhy, M.Kover et al., *Materials and qTechnology*, **49**, 213 (2015).
http://mit.imt.si/Revija/izvodi/mit152/kubina.pdf
20. J.Gubicza, N.H.Nam, L.Balogh et al., *Journal of Alloys and Compounds*, **378**, 248 (2004).
https://www.sciencedirect.com/science/article/abs/pii/S0925838804000945.
21. D.V.Pavlenko, D.V.Tkach, S.M.Danilova-Tret'yak, L.E.Evseeva, *Journal of Engineering Physics and Thermophysics*, **90**, 685 (2017). doi:10.1007/s10891-017-1616-8
22. J.J.Kearns, https://ntrl.ntis.gov/NTRL/dashboard/searchResults/titleDetail/WAPDTM472.xhtml.
23. V.Grytsyna, D.Malykhin, T.Yurkova et al., *East Eur. J. Phys.*, **3**, 38 (2019).
https://doi.org/10.26565/2312-4334-2019-3-05
24. V.I.Vishnyakov, A.A.Babareko, S.A.Vladimirov, I.V.Egiz, Theory of Texture Formation in Metals and Alloys, Nauka, Moscow (1979) [in Russian].
https://kundoc.com/queue/pdf-physical-properties-of-crystals-their- representation-by-tensors-and-matrices-.html.
25. J.F.Nye, Physical Properties of Crystals their Representation. Their Representation by Tensors and Matrices, University Press, Oxford (2006).
http://93.174.95.29/main/7258F1CE1EEE4CD628566F4EA21CDD58
26. K.W.Andrews, D.J.Dyson, S.R.Keown, Interpretation of Electron Diffraction Patterns, Springer, Boston, MA (1967).
https://doi.org/10.1007/978-1-4899-6475-5_2.
27. B.S.Karpinos, D.V.Pavlenko, O.Ya.Kachan, *Strength of Materials*, **44**, 100 (2012).
https://link.springer.com/article/10.1007/s11223-012-9354-9
28. J.S.Weaver, M.W.Priddy, D.L.McDowell, S.R.Kalidindi, *Acta Materialia*, **117**, 23 (2016).
http://dx.doi.org/10.1016/j.actamat.2016.06.053
29. J.Gong, A.Wilkinson, *Philosophical Magazine Letters*, **90**, 503 (2010).
http://dx.doi.org/10.1080/09500831003772989.
30. J.-M.Zhang, Y.Zhang, K.-W.Xu, V.Ji, *Thin Solid Films*, **515**, 7020 (2007). URL:
https://doi.org/10.1016/j.tsf.2007.01.045.
31. D.Tromans, *International Journal of Research and Reviews in Applied Sciences*, **6**, 462 (2011).
https://www.arpapress.com/volumes/vol6issue4/ijrras_6_4_14.pdf
32. J.Lemaitre, R.Desmorat, M.Sauzay, *Eur. J. Mech. A*, **19**, 187 (2000)._
https://www.sciencedirect.com/science/article/pii/S0997753800001613.
33. F.K.Mante, G.R.Baran, B.Lucas, *Biomaterial*, **20**, 1051 (1999).
https://www.sciencedirect.com/science/article/pii/S0142961298002579.
34. S.V.Lubenets, A.V.Rusakova, L.S.Fomenko, V.A.Moskalenko, *Low Temp. Phys.*, **44**, 73 (2018).
https://doi.org/10.1063/1.5020901.
35. E.Merson, R.Brydson, A.Brown, *Journal of Physics*, **Conference Series 126**, 012020 (2008).
https://iopscience.iop.org/article/10.1088/1742-6596/126/1/012020/pdf.
36. C.Zambaldi, Y.Yang, T.R.Bieler, D.Raabe, *J. Mater. Res.*, **27**, 356 (2012).
https://doi.org/10.1557/jmr.2011.334

37. M.W.Priddy, D.L.McDowell, S.R.Kalidindi, *Acta Materialia*, **117**, 23 (2016). http://dx.doi.org/10.1016/j.actamat.2016.06.053.
38. P.Zhang, S.X Li., Z.F.Zhang, *Materials Science and Engineering A*, **529**, 62 (2011). https://doi.org/10.1016/j.msea.2011.08.061.
39. F.Khodabakhshi, M.Haghshenas, H. Eskandari, B.Koohbor, *Materials Science & Engineering A*, **636**, 331 (2015). http://dx.doi.org/10.1016/j.msea.2015.03.122
40. D.Pavlenko, Y.Dvirnyk, R.Przysowa, *Advanced Materials and Technologies for Compressor Blades of Small Turbofan Engines. Aerospace*, **8**, 1 (2021). https://www.mdpi.com/2226-4310/8/1/1/htm